

Redesigning the Substrate Specificity of ω -Aminotransferase for the Kinetic Resolution of Aliphatic Chiral Amines

Byung-Kwan Cho,^{1,2} Hyung-Yeon Park,³ Joo-Hyun Seo,^{1,2} Juhan Kim,^{1,2}
Taek-Jin Kang,^{1,2} Bon-Su Lee,³ Byung-Gee Kim^{1,2}

¹School of Chemical and Biological Engineering, Seoul National University, Seoul 151-742, Korea; telephone: +82-2-880-6774; fax: +82-2-883-6020; e-mail: byungkim@snu.ac.kr

²Institute of Molecular Biology and Genetics, Seoul National University, Seoul 151-742, Korea

³Department of Chemistry, Inha University, Incheon, Korea

Received 1 February 2007; revision received 20 June 2007; accepted 9 July 2007

Published online 6 August 2007 in Wiley InterScience (www.interscience.wiley.com). DOI 10.1002/bit.21591

ABSTRACT: Substrate specificity of the ω -aminotransferase obtained from *Vibrio fluvialis* (ω -ATVf) was rationally redesigned for the kinetic resolution of aliphatic chiral amines. ω -ATVf showed unique substrate specificity toward aromatic amines with a high enantioselectivity ($E > 100$) for (S)-enantiomers. However, the substrate specificity of this enzyme was much narrower toward aliphatic amines. To overcome the narrow substrate specificity toward aliphatic amines, we redesigned the substrate specificity of ω -ATVf using homology modeling and the substrate structure-activity relationship. The homology model and the substrate structure-activity relationship showed that the active site of ω -ATVf consists of one large substrate-binding site and another small substrate-binding site. The key determinant in the small substrate-binding site was D25, whose role was expected to mask R415 and to generate the electrostatic repulsion with the substrate's α -carboxylate group. In the large substrate-binding site, R256 was predicted to recognize the α -carboxylate group of substrate thus obeying the dual substrate recognition mechanism of aminotransferase subgroup II enzymes. Among the several amino acid residues in the large substrate-binding site, W57 and W147, with their bulky side chains, were expected to restrict the recognition of aliphatic amines. Two mutant enzymes, W57G and W147G, showed significant changes in their substrate specificity such that they catalyzed transamination of a broad range of aliphatic amines without losing the original activities toward aromatic amines and enantioselectivity.

Byung-Kwan Cho's present address is Department of Bioengineering, University of California-San Diego, 9500 Gilman Dr., La Jolla, CA 92093.

Juhan Kim's present address is Cooperative Institute for Research in Environmental Sciences, University of Colorado, Boulder, CO 80309.

Taek-Jin Kang's present address is Research Center for Advanced Science and Technology, University of Tokyo, 4-6-1 Komaba, Meguro-ku, Tokyo 153-8904, Japan. Correspondence to: Byung-Gee Kim, School of Chemical and Biological Engineering, Seoul National University, Seoul 151-742, Korea.

Contract grant sponsor: 21C Frontier Microbial Genomics and Applications

Contract grant sponsor: Center Programs from the Ministry of Science & Technology

Contract grant sponsor: Nano Bioelectronics & Systems Research Center in Seoul National University

Biotechnol. Bioeng. 2008;99: 275–284.

© 2007 Wiley Periodicals, Inc.

KEYWORDS: aminotransferase; chiral amine; homology modeling; substrate specificity

Introduction

Chiral amines are often used as building blocks in the synthesis of neurological, cardiovascular, immunological, anti-hypertensive, anti-infective, and anti-emetic drugs as well as chiral auxiliaries for asymmetric chiral induction and as resolving agents for the preparation of optically pure carboxylic acids (Gutman et al., 1992; Kitaguchi et al., 1989). Owing to the great usefulness and versatility of these compounds, many optically active chiral amines have been prepared by asymmetric synthesis, deracemization, fractional crystallization, and kinetic resolution using chemical and/or enzymatic methods (Alexeeva et al., 2002; Balint et al., 2001; Cho et al., 2003b; Oehrner et al., 1996; Sheldon 1996; Shin and Kim 1999). Among several enzymatic approaches employed for the synthesis of optically active amines, the aminotransferase system is a promising one because of its broad substrate specificity, high enantioselectivity, and high turnover number as well as no requirement for external cofactor regeneration (Cho et al., 2003a,c; Shin et al., 2003; Stewart 2001; Taylor et al., 1998).



ω -Aminotransferase (ω -ATVf) cloned from *Vibrio fluvialis* JS17 is a unique pyridoxal 5'-phosphate (PLP) dependent enzyme that catalyzes the amino group transfer reaction from an amine to a keto acid (or an aldehyde) in a reversible manner (Shin et al., 2003). ω -ATVf showed a high enantioselectivity ($E > 100$) for (*S*)-enantiomer of the chiral amines and had distinctive substrate specificity for chiral aromatic amines such as (*S*)-1-phenylethylamine. However, the narrow substrate specificity of ω -ATVf restricts its application for the kinetic resolution of aliphatic amines (Shin and Kim 2002).

Two approaches have mainly been used for the expansion of the substrate specificity of aminotransferase; rational protein design and directed enzyme evolution (Stemmer 2002; Tindbaek et al., 2004). One of the notable successes of the rational protein design approach was the conversion of *E. coli* aspartate aminotransferase into an aromatic amino acid aminotransferase by site-specific mutations (Malashkevich et al., 1995). On the other hand, the directed evolution (Chen, 2001) relying on random mutation to rapidly screen improved strains of target properties has been used to convert the *E. coli* aspartate aminotransferase into a branched chain amino acid aminotransferase (Oue et al., 1999; Yano et al., 1998) and to relieve the product inhibition of ω -ATVf (Yun et al., 2005). To use the rational protein design, a correct protein structural coordinate is a prerequisite to identify the amino acid residues having roles in the recognition of substrates. However, if the structure of a protein is not available, but its sequence shows high sequence similarity with known protein structures, homology modeling could be used as a powerful tool to predict the unknown target protein structure based on the known protein structures (Baker and Sali 2001; Marti-Renom et al., 2000). Although the homology model can provide general information to guide the possible mutations to engineer the protein (Harel et al., 1992; Liu et al., 1997; Siezen et al., 1991), it is not that easy to reveal the exact interactions of each residue with only homology modeling.

In the previous studies, we have described the production of optically active chiral amines using ω -ATVf via kinetic resolution and reported its active site model based on the substrate structure-activity relationship (Shin and Kim, 2002). The substrate structure-activity relationship suggested that the active site of ω -ATVf consists of one large and another smaller pocket. The key determinants for the recognition of the substrates are the difference in the size of each binding pocket, and the electrostatic repulsion of the carboxylic group of the substrates in the small pocket. Herein, we report the confirmation of the previous structure-activity relationship based upon the experiments, and significant alterations in the substrate specificity of the ω -ATVf by rational design using data from the homology modeling and the relationship between substrate structures and the enzyme activity. The enzyme was successfully redesigned to accept the chiral aliphatic amines without losing its substrate specificity for the aromatic chiral amines and (*S*)-specific enantioselectivity.

Materials and Methods

Chemicals

The chemicals required for protein assay and sodium dodecyl sulfate–polyacrylamide gel electrophoresis (SDS–PAGE) were from Bio-Rad (Hercules, CA). Restriction endonucleases used for DNA manipulation were obtained from Boehringer Mannheim GmbH (Mannheim, Germany). *E. coli* BL2 (DE3) for the protein overexpression was purchased from Novagen (Madison, WI). [¹⁴C] leucine (11.7 GBq/mmol, 1.85 MBq/mL) was obtained from Amersham Biosciences (Piscataway, NJ). Other reagents used in cell-free protein synthesis were purchased from Wako Pure Chemicals (Osaka, Japan). Chiral amines, isopropyl- β -D-thio-galactopyranoside (IPTG), amines, amino acids, α -keto acids, and antibiotics were from Sigma-Aldrich (St. Louis, MO). Luria-Bertani broth was from Difco Laboratories (Detroit, MI). All other reagents were of analytical grade and were obtained from commercial sources.

Construction of Plasmids

The pET24ma (constructed by Dr. David Sourdivé, Pasteur Institute, France) containing a p15A replication origin was used for the construction of the plasmids carrying the ω -ATVf gene. The structural gene of the ω -ATVf was amplified from the genomic DNA of *V. fluvialis* JS17 by PCR using the previously determined primers having *Nde*I and *Hind*III restriction sites (Shin et al., 2003). The amplified gene was digested by *Nde*I and *Hind*III, and the digested fragment coding for the ω -ATVf was inserted into the pET24ma cut with the same restriction enzymes. To obtain recombinant strain harboring the ω -ATVf, the plasmid carrying the ω -ATVf gene was transformed into the *E. coli* BL21 (DE3) and selected for kanamycin (25 μ g/mL) resistance.

Computational Methods

ClustalW and GeneDoc were used to generate and to edit the multiple alignment of ω -ATVf (Nicholas et al., 1997; Thompson et al., 1994). Sequence alignment was performed with BLOSUM62 substitution matrix by using default gap initiation and an extension penalty. For the determination of the relatedness of ω -ATVf with other aminotransferases, a profile analysis algorithm was used (Eddy, 1998). The 32 selected aminotransferase sequences could be divided into four subgroups based on their mutual similarities in primary structure (Mehta et al., 1993). The subgroup-specific profiles were built from the multiple alignment of each subgroup by HMMER version 2.2 (<http://hmmer.wustl.edu>). The homology model of ω -ATVf was constructed using the structure of 2,2-dialkylglycine decarboxylase (PDB code 1DGE) as a template with Composer and Genefold[®] module in SYBYL 6.8 (St. Louis, MO). The PLP molecule

was taken from the 2,2-dialkylglycine decarboxylase structure, and inserted into the model as a hetero atom during the homology modeling. Manual adjustments were made to remove steric clashes of the side chain torsion angles of residues using Homology module in SYBYL 6.8. The calculation of accessible surface area of substrates was carried out with SYBYL 6.8. The initial structures of substrates were energy-minimized using conjugate gradient minimization until the maximum derivatives were less than 0.001 kcal/mol/Å. In all minimizations, a cutoff distance of 11 Å was used with Tripos Force Field using the Gasteiger–Huckel charge. Based on the energy-minimized conformation of the substrates, solvent-accessible areas of R1 and R2 groups were calculated using Connolly's method with a probe size of 1.4 Å.

Site-Directed Mutagenesis

Mutations were introduced into the expression vector pET24ma containing the ω -ATVf gene using the Quick-change™ site-directed mutagenesis kit from Stratagene (La Jolla, CA). The PCR amplifications and *E. coli* transformations were carried out according to the manufacturer's instructions. The mutations were verified by DNA sequencing.

Expressions of Wild and Mutant Enzymes

E. coli BL21 (DE3) strains harboring the plasmids were grown at 37°C in 50 mL Luria-Bertani broth supplemented with 25 µg/mL kanamycin. Expression of the mutated and the wild-type of ω -ATVf were initiated by induction with IPTG (1 mM) when the cultures reached absorbance of 0.6 at 600 nm. After 6 h from induction, the cells were harvested by centrifugation at 4,000 rpm for 15 min at 4°C. The cells were washed twice with 25 mL of ice-cold 50 mM Tris-HCl buffer (pH 7.2). Finally, the cells were resuspended using 5 mL of the sonication buffer consisting of 50 mM Tris-HCl buffer (pH 7.2), 20 µM pyridoxal 5'-phosphate, 2 mM EDTA, 1 mM PMSF, 10% (w/v) glycerol, and 0.01% (v/v) 2-mercaptoethanol. The cells were disrupted by sonication maintaining the temperature constant in an ice-bath. Cell debris was removed by centrifugation at 13,000 rpm for 20 min at 4°C and the resulting supernatant was dialyzed against 1 L of the dialysis buffer composed of 50 mM Tris-HCl buffer (pH 7.2), 20 µM pyridoxal 5'-phosphate, 0.2 mM EDTA, 1 µM PMSF, 10% (w/v) glycerol, and 0.001% (v/v) 2-mercaptoethanol. The dialyzed cell extracts were stored at -70°C for further study.

Cell-Free Protein Synthesis

Each ω -ATVf mutant was over-expressed in *E. coli* BL21 (DE3), and the expression levels of wild-type and mutant ω -ATVf were evaluated by SDS-PAGE (data not shown). Although the expression levels in *E. coli* BL21 were high enough to measure their activities, the amount of the

enzymes used in the reaction should be measured correctly to compare the relative reactivity of the mutant enzymes. For that purpose, we used the cell-free protein synthesis system to quantify the each protein (Jewett and Swartz, 2004; Kang et al., 2002). The cell-free protein synthesis reaction was carried out using *E. coli* S30 (Kang et al., 2002). The amount of proteins synthesized by cell-free protein synthesis system were measured by the incorporation of [¹⁴C]leucine into the proteins using a liquid scintillation counter (Kang et al., 2002). To determine the final soluble protein yield synthesized, 30 µL of the reaction mixture was centrifuged at 12,000 rpm for 15 min at 4°C. Ten microliters of the supernatant were combined with 100 µL of 0.1 N NaOH, and TCA precipitation was carried out as described elsewhere (Jewett and Swartz, 2004). Although the amounts of in vitro synthesized ω -ATVf varied significantly from lot to lot, the specific activities could easily be calculated using a simple regression method. The amounts of wild-type, W57G and W147G ω -ATVf synthesized were 79.1, 88.8, and 94.8 µg/mL, respectively. Due to the lack of ω -ATVf activity in *E. coli* S30 extract, the enzymes synthesized with cell-free system could be used for the reaction without further purification. Using (S)-1-phenylethylamine and pyruvate as respective amino donor and amino acceptor, the specific activities of wild-type enzyme and those of mutants W57G and W147G ω -ATVf were 0.079, 0.165, and 0.082 µM/mg·s, respectively, showing that W57G and W147G showed 2.08- and 1.04-fold higher activity than the wild-type ω -ATVf in (S)-1-phenylethylamine and pyruvate pair reactions. The result indicates that the mutations do not reduce the original reactivity toward (S)-1-phenylethylamine and pyruvate.

Enzyme Activity Assay

The reaction was started by addition of the dialyzed cell extracts or the mixture of in-vitro translated ω -ATVf at 37°C. To investigate substrate specificity, 0.5 mL of assay mixture containing 100 mM Tris-HCl (pH 8.0), 5 mM amine, and 20 mM pyruvate was used. The reaction was started by addition of the ω -ATVf, and consumption of pyruvate was measured at 210 nm after stopping the reaction by 0.5 mL of 16% perchloric acid using a HPLC system (Younglin, Korea) equipped with an Aminex column (Bio-Rad). The loaded reaction mixture on the column was eluted with isocratic 5 mM sulfuric acid at 40°C. In the case of the in-vitro translated ω -ATVf, 0.1 mL of the same assay mixture was used to measure the substrate specificity.

Results and Discussion

Homology Modeling of ω -ATVf to Predict the Active Site Amino Acid Residues

To select a template structure for the homology modeling, the primary structure of ω -ATVf was compared with other aminotransferases using family profile analysis and sequence

alignment (Eddy, 1998; Gribskov et al., 1987). The normalized log-odd score of ω -ATVf calculated by the family profile of aminotransferase subgroup II (Cho et al., 2006; Mehta et al., 1993) showed a high positive value (profile score = 194.4), whereas the values based on the family profiles of the other aminotransferase subgroups were negative values (profile score of subgroup I = -197.2; profile score of subgroup III = -198.6; profile score of subgroup IV = -261.0). This result suggested that the ω -ATVf is one of the aminotransferase subgroup II enzymes, whose members are ornithine aminotransferase (Orn-AT, EC 2.6.1.13), 4-aminobutyrate aminotransferase (GABA-AT, EC 2.6.1.19), DAPA aminotransferase (DAPA-AT, EC 2.6.1.62), glutamate-1-semialdehyde aminotransferase (GSA, EC 5.4.3.8), and 2,2-dialkylglycine decarboxylase (DGD, EC 4.1.1.64) (11, 15, 21, 24). Among the subgroup II members, sequence alignment using Genefold[®] yielded DGD (PDB entry: 1DGE) as the plausible template, which has the highest similarity with ω -ATVf.

As another selection criterion, the molecular structures of substrates of aminotransferase subgroup II enzymes were compared to each other as shown in Table I. The substrates of DGD (i.e., 2,2-dialkylglycine and pyruvate) are close to those of ω -ATVf substrates (i.e., 1-phenylethylamine and pyruvate), except carbon dioxide and benzyl ring. The molecular structures of the substrates of other aminotransferases in the subgroup II are quite different from those of ω -ATVf. Firstly, ω -ATVf and DGD use pyruvate as amino acceptor, whereas other subgroup II enzymes use α -ketoglutarate or special amino acceptors (i.e., 8-amino-7-

oxononanoic acid for DAPA-AT, 3-amino-4-oxovaleric acid for GSA) in the forward reaction. Secondly, while ω -ATVf and DGD use ketones (i.e., acetophenone and acetone) as amino acceptor in the backward reaction, other enzymes in the subgroup II use keto acids. This indicates that several amino acid residues having similar functional groups to interact with the substrates would be conserved in the active sites of both enzymes. Therefore, the homology model of the ω -ATVf was constructed with the structure of DGD (PDB entry: 1DGE). Figure 1 shows the important active site residues positioned in large (L) and small (S) substrate-binding sites around the PLP-substrate Schiff base with (S)-1-phenylethylamine or pyruvate.

Identification of PLP-Anchoring Residues

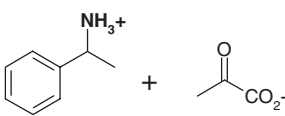
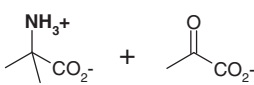
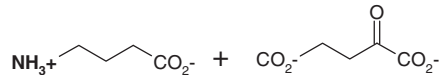
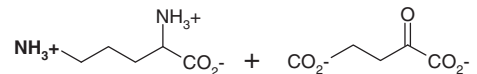
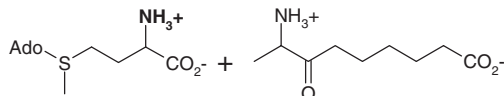
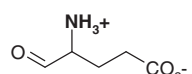
In all four subgroups of aminotransferase, only four amino acid residues are invariant (Mehta et al., 1993). Of those invariant residues, three amino acid residues interact with PLP molecule in the active site. One of them is a lysine residue, which immobilizes PLP molecule via Schiff base formation in the active site, and is well conserved (K285) in the ω -ATVf. To investigate the role of K285 on the formation of Schiff base with PLP molecule, a mutant was generated by changing the residue to histidine. The enzymatic activity was then quantitatively measured using the cell-free synthesized mutant enzyme. As expected, the enzymatic activity of K285H mutant did not show the transamination activity between (S)-1-phenylethylamine and pyruvate.

The phosphate moiety of PLP was predicted to form hydrogen bonds with Y150, S118, and G152. As the second invariant residue, G152 is located at the domain interface and forms salt bridge and hydrogen bond to PLP (Mehta et al., 1993). The N1 atom of PLP can also form an ion pair with carboxylate group of D256, which is the third invariant residue in all the aminotransferases. Similar to the K285H, the D256A mutant lost its activity on the transamination, indicating that the transamination occurs in the same way as in other aminotransferases with the assistance of K285 and D256 (Mehta et al., 1993).

Rationales of Protein Design to Broaden Substrate Specificity

Previous studies on the substrate structure-activity relationship suggested two important findings for this enzyme: (1) there is an electrostatic repulsion between α -carboxylate group of the substrates and amino acid residues in the small substrate-binding site, which prevents any chiral amines containing α -carboxylate group from entering the active site as an amino donor, and (2) the dual mode for the recognition of both hydrophobic and carboxylate groups in the large substrate-binding site is a key determinant controlling its substrate specificity and enantioselectivity (Shin and Kim, 2002). To elucidate the key residues in the proposed large and small substrate-binding sites, the

Table I. Substrates of aminotransferase subgroup II.

Enzyme	Substrates ^a
ω -ATVf	
DGD	
GABA-AT	
Orn-AT	
DAPA-AT	
GSA	

^aThe reactive amino group of each substrate is in bold.

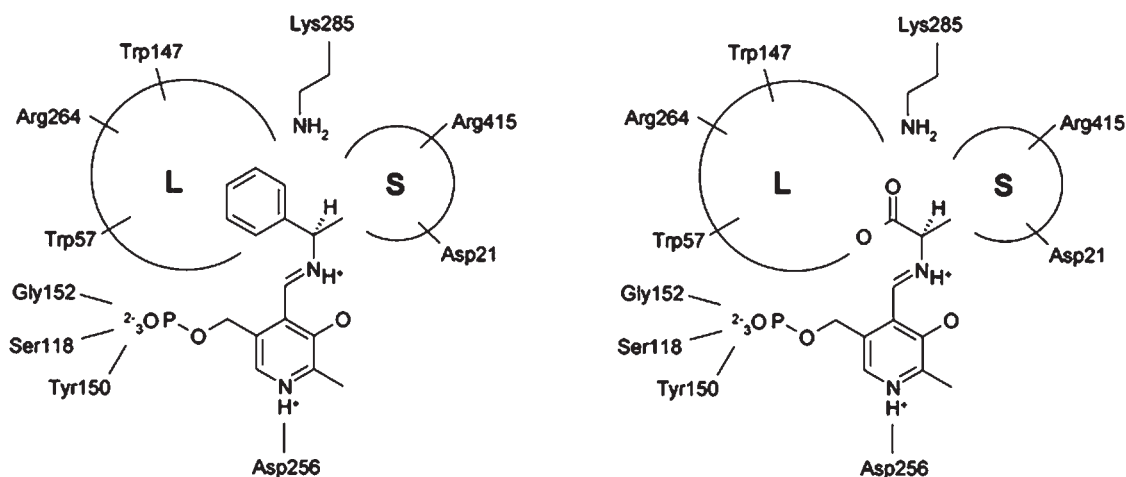


Figure 1. Predicted active site of ω -ATVf by substrate structure-reactivity relationships and homology model. The structures are the external aldimine formed by transaldimination stage, the attack of the substrate's deprotonated amino group on C4' of the PLP, and displacement of the lysine ϵ -NH₂ group from the internal Schiff base. L and S indicate the large substrate-binding site and the small substrate-binding site, respectively.

docking of (*S*)-1-phenylethylamine and pyruvate into the predicted active site of the homology model of ω -ATVf (Fig. 1; Kramer et al., 1999; Rarey et al., 1996). The docking simulation indicated that among the several key residues in the large substrate-binding site, W57 and W147 interact with the aromatic group of (*S*)-1-phenylethylamine via hydrophobic interactions. The proposed large substrate-binding site is also able to recognize the α -carboxylate group of pyruvate by R264 residue through ionic interaction and/or hydrogen bonding.

The key issue for broadening amino donor substrate specificity without losing its original substrate specificity would be either by enlarging the large substrate-binding site to accept the amines of larger size or by changing the local chemical environment to accept other functional groups. To allow aliphatic amines of larger size as well as aromatic amines as amino donor, mutations of the two tryptophan residues to glycines were designed to remove the geometrical hindrance and to allow a larger substrate-binding site. It was expected that the mutations not only alter the direct contacts between the ω -ATVf and substrate but also promote the flexibility of the large substrate-binding site of the enzyme. However, R264 in the large substrate-binding site was kept to maintain the interaction with α -carboxylate group of pyruvate.

Substrate Recognition in the Substrate-Binding Sites

For the recognition of the α -carboxylate group of pyruvate, it is noteworthy that ω -ATVf has R415, which is another well conserved amino acid residue among all aminotransferases and known to bind to α -carboxylate group of the substrate via a salt bridge and a hydrogen bond (Liu et al., 2004). The

replacement of the arginine residues of other aminotransferases by a lysine, histidine, alanine, tyrosine, or phenylalanine showed a drastic reduction in the enzymatic activity (Eliot et al., 2002; Liu et al., 2004; Markova et al., 2005; Storici et al., 1999). Since the arginine residue largely determines the orientation of the substrate moiety relative to the plane of the PLP-substrate imine, the enzymatic activity decreased in the mutants (Hirotzu et al., 2005). The aminotransferase subgroup II enzymes such as Orn-AT and GABA-AT have dual substrate specificity, in the sense that it can transfer the amino group of both primary amines and α -amino acids (Liu et al., 2004; Markova et al., 2005; Storici et al., 1999). This particular aspect of the substrate specificity is due to the two arginine residues that interact with α -carboxylate and the side chain carboxylate of the substrate, respectively (Markova et al., 2005). In the case of Orn-AT, while α - and γ -carboxylate group of glutamate are recognized by R413 and R180, respectively, the α -carboxylate group of ornithine is bound to R180 (Markova et al., 2005). The interaction between the α -carboxylate group of ornithine and R180 is important in positioning the ornithine to lead to transamination of the ω -amino group (Markova et al., 2005). The crystal structure of the Orn-AT-inhibitor complex showed that E235 can mask the conserved arginine (R413) via tight hydrogen bonding and salt bridge interactions from the binding of the α -carboxylate group of ornithine (Markova et al., 2005). Similarly, it was predicted that the α -carboxylate group of pyruvate interacts with R264 in the large substrate-binding site instead of R415 in the small substrate-binding site of ω -ATVf. Interestingly, the replacement of the R415 residue of ω -ATVf by lysine did not result in any reduction in transamination activity (Table II), thus supporting the fact that the α -carboxylate group of the substrate is not recognized by R415, but by R264 in the large

Table II. Substrate specificity of wild-type and R415L mutant.

Substrate	Relative specific activity (μ_{rel} , %) ^a	
	Wild-type	R415L
(S)-1-phenylethylamine	100.0	168.2
(S)-Aminophenylacetate	ND ^b	97.4
(S)-Phenylalanine	ND	5.8
(S)-2-Amino-4-phenylbutyrate	ND	ND
Pyruvate	100.0	135.2
Oxophenylacetate	<0.1	94.6
2-oxo-3-phenylpropionate	<0.1	13.8
2-oxo-4-phenylbutyrate	ND	ND

^aThe reaction conditions for the calculation of specific activities were as follows: 0.1 mL of reaction media consists of 50 mM Tris-HCl (pH 7.2), 5 mM (S)-amines or (S)-amino acids, 10 mM pyruvate and 10 μ L cell-free synthesized wild-type and mutant ω -ATVf at 37°C. For the amino acceptors, 0.1 mL of reaction media consists of 50 mM Tris-HCl (pH 7.2), 5 mM (S)-1-phenylethylamine, 10 mM amino acceptors and 10 μ L cell-free synthesized wild-type and mutant ω -ATVf at 37°C. Relative specific activities (μ_{rel}) for amino donors and acceptors were calculated based upon the specific activity for (S)-1-phenylethylamine and pyruvate, respectively.

^bND stands for “not detected.”

substrate-binding site. As another determinant in the small substrate-binding site, D21 was predicted to have the similar role with the E235 of Orn-AT. Although it can be expected that pyruvate binds to the active site by forming a hydrogen bond and a salt bridge between its α -carboxylate group and R415, D21 possibly masks the R415 residue and/or makes electrostatic repulsion with the α -carboxylate group of the substrates. Therefore, the C_{α} -hydrogen of (S)-1-phenylethylamine in the active site is toward the *si* face at C4' of the conjugated π -system of the internal aldimine, and the abstraction of the α -proton occurs from the *si* face. Then, a proton would be preferably added from the *si* face during the amination step, indicating that the carboxylate group of pyruvate should be positioned in the large substrate-binding site and recognized by the R264 residue instead of the R415.

Substrate Specificities Toward Aromatic Amines

With the result of homology modeling, the steric hindrance caused by W57 and W147 residues in the proposed large substrate-binding site was identified as the major reason for the limited substrate specificity of ω -ATVf. Therefore, we tried to remove these structural barriers by changing the residues to smaller amino acids. Two mutants, W57G and W147G ω -ATVf, were made by changing one of the residues into glycine, and expressed by cell free translation. As the mutants did not show any reduction in the original activity of the transaminase toward aromatic amines, we further examined the changes in the substrate specificities of these two mutants.

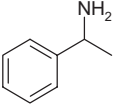
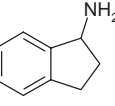
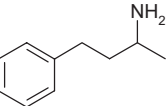
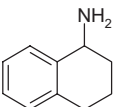
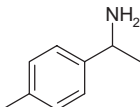
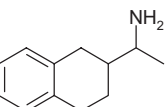
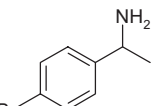
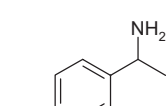
To examine the alteration of the substrate specificities of ω -ATVf mutants by a single amino acid change, three sets of

amino donor substrates were used. The amino donor substrates were the methyl amines containing (1) aromatic side chain (R1) and methyl side chain (R2) (substrate group I, **A**); (2) aromatic side chain (R1) and hydrogen (R2) (substrate group II, **B**); and (3) aliphatic side chain (R1) and methyl side chain (R2) (substrate group III, **C**). Relative activities (μ_{rel}) for the amino donor were measured using pyruvate as a fixed amino acceptor and compared with that of (S)-1-phenylethylamine (Tables III–V). To prevent substrate inhibition, 5 and 10 mM of the amino donor and pyruvate were used. The amounts of enzymes used in the reactions were adjusted after the cell-free protein synthesis.

The result showed that W57G and W147G ω -ATVf accept the group I substrates with large accessible areas better than wild-type ω -ATVf, as predicted (Tables III and IV). In the amino donor specificity of wild-type ω -ATVf toward substrate group I, the increase in the size of the R1 resulted in lower reactivity (A3, A5–A8) compared with A1. Similarly, the increase in the size of the R1 of the substrate group II resulted in the decrease in the reactivity (B1–B4). W147G mutation slightly increased the enzymatic activities for the amino donor substrates we have examined, whereas W57G mutation greatly increased its enzymatic activities for the same substrates. For example, W57G ω -ATVf showed 3.6- and 2.3-fold higher reactivities with A2 and A4. With the substrates with larger accessible surface area, it showed much higher reactivity: 9.4-fold (A3) and 19.8-fold (A6) higher reactivities than wild-type enzyme. In the case of substrate group II (B1–B4), W57G ω -ATVf showed 2.5-fold (B1) to 40.6-fold (B4) higher activity than wild-type ω -ATVf as shown in Table IV. Even in the case of W147G mutation, similar relationships between the size of R1 and relative specific activity were observed.

The changes in the relative specific activity of W57G and W147G ω -ATVf became less sensitive to the changes in the accessible surface area than wild-type ω -ATVf (Fig. 2A,B). This suggested that W57G and W147G mutants have broader substrate specificity even within the substrate groups I and II compared with wild-type ω -ATVf. The transamination is composed of two half reactions. Therefore, in the reactions catalyzed by ω -ATVf, both substrate specificities (i.e., $k_{cat}/K_m^{aminodonor}$ and $k_{cat}/K_m^{pyruvate}$) should be considered together to understand the structural changes in the active site of aminotransferase in detail. Since the amino acceptor was fixed to pyruvate in the above experiments, the changes in the relative activity indicated the changes in the ratio of $k_{cat}/K_m^{aminodonor}$ of the mutants to that of the wild-type. Therefore, the effect of structural changes can be explained by the slope changes in the ratio of relative specific activity (μ_{rel}) to accessible surface area. Judging from the tendency of the changes in the reactivity, W57G and W147G mutations seemed to open the cavity through the adjustment of hydrophobic interaction for positioning of the aromatic group in the large substrate-binding site, which results in efficient catalysis of the aromatic amines without loss of its original reactivity.

Table III. Substrate specificity of wild-type and mutant ω -ATVf toward substrate group I.

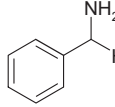
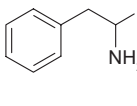
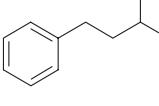
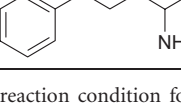
Substrate	Relative specific activity (μ_{rel} , %) ^a		
	W57G	W147G	Wild-type
A1 	208.9	103.8	100.0
A2 	567.8	146.9	156.5
A3 	511.4	46.1	54.2
A4 	286.6	99.3	123.6
A5 	118.0	48.6	35.1
A6 	83.1	48.9	4.2
A7 	236.3	65.7	45.3
A8 	192.4	40.4	29.4

^aThe reaction condition for the calculation of specific activity was as following: 0.1 mL of reaction media consists of 50 mM Tris-HCl (pH 7.2), 5 mM racemic amines, 10 mM pyruvate and 10 μ L cell-free synthesized wild-type and mutant ω -ATVf at 37°C. Relative specific activities (μ_{rel}) for the amino donor were calculated based upon the specific activity for (S)-1-phenylethylamine.

Alteration of Substrate Specificities Toward Aliphatic Amines

The relative specific activities of mutant enzymes toward substrate group III were compared to those of wild-type enzyme (Table V). Wild-type ω -ATVf showed the highest activity for C6, suggesting that the size of large substrate-binding site becomes an important parameter in determining the relative reactivity of substrates. Wild-type ω -ATVf

Table IV. Substrate specificity of wild-type and mutant ω -ATVf toward substrate group II.

Substrate	Relative specific activity (μ_{rel} , %) ^a		
	W57G	W147G	Wild-type
B1 	290.6	106.2	115.6
B2 	133.3	76.7	23.4
B3 	163.9	65.2	19.7
B4 	146.4	51.5	3.6

^aThe reaction condition for the calculation of specific activity was as following: 0.1 mL of reaction media consists of 50 mM Tris-HCl (pH 7.2), 5 mM amines, 10 mM pyruvate and 10 μ L cell-free synthesized wild-type and mutant ω -ATVf at 37°C. Relative specific activities (μ_{rel}) for amino donor were calculated based upon the specific activity for (S)-1-phenylethylamine.

showed much lower reactivity for C5 (23.4%) and C6 (24.4%) than the reactivity for A1, however, W57G mutation improved the reactivity for C5 and C6, resulting in 75.3% and 171.3% reactivities compared to the reactivity for A1, respectively. W57G ω -ATVf showed 5.1-fold (C4) to 19.2-fold (C1) higher activities than wild-type ω -ATVf, whereas W147G ω -ATVf showed 0.9-fold (C4) to 6.1-fold (C1) higher activities than wild-type ω -ATVf. In the amino donor specificity of wild-type ω -ATVf toward the substrate group III, the increase in the size of the R1 resulted in the higher reactivities for all the compounds (C1–C6) we have examined. W57G ω -ATVf exhibited a significant increase in the reactivities for the substrate group III; 1-methyl-hexylamine (C5) and 1,5-dimethyl-hexylamine (C6) showed 6.7- and 14.7-fold increases, respectively. Other aliphatic amines (C1–C4) showed 19.2-, 11.1-, 7.4-, and 5.1-fold increases in the reactivity, respectively (Table V). In the case of W147G mutation, its enzymatic activities toward aliphatic amines were similar to those of wild-type ω -ATVf except C1.

As shown in Figure 3, the slope of the changes in the relative specific activity (μ_{rel}) of the two mutants (i.e., W57G and W147G ω -ATVf) to the accessible surface area becomes positive and lower than that of wild-type ω -ATVf. Moreover, the reactivities of the substrate group III are similar to those of the substrate groups I and II, suggesting that W57G and W147G ω -ATVf have a substrate binding site sufficient to locate aliphatic amine as well as aromatic amines. The positive slope of the changes in the ratio of

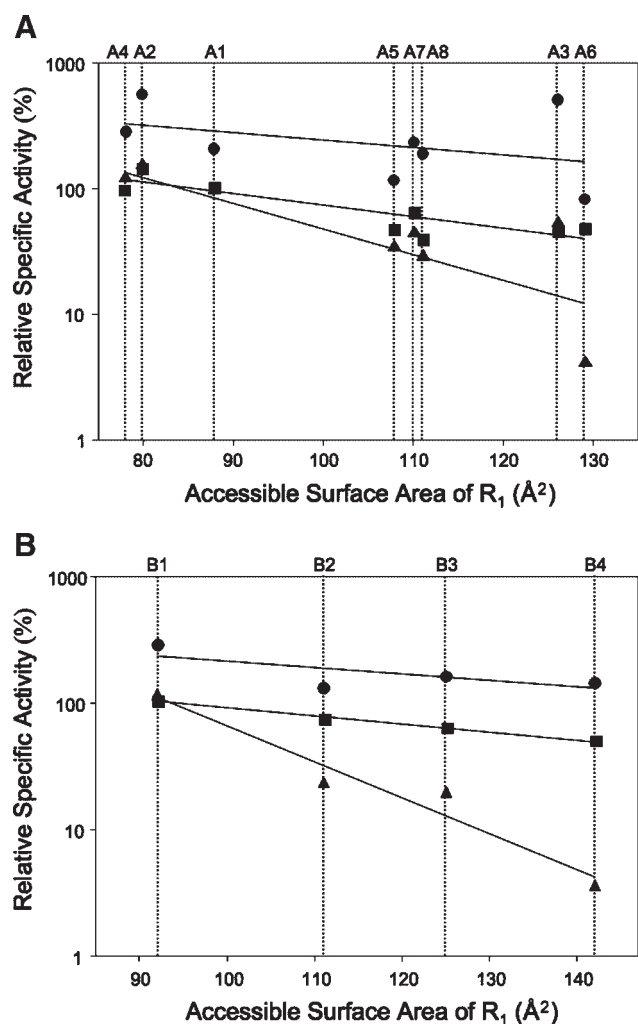


Figure 2. Relationships between the accessible surface area of substrate group I (A) and II (B) and the activity of the ω -ATVf (●, W57G ω -ATVf; ■, W147G ω -ATVf; ▲, wild-type ω -ATVf).

relative specific activity (μ_{rel}) to the accessible surface area indicates that hydrophobic interactions exist between the large substrate-binding site of the E-PLP and R1 group (Shin and Kim, 2002), and the lower slope displays that the hydrophobic interaction is adjusted by well-positioning of the substrates in the large substrate-binding site.

Conclusion

To make ω -ATVf a more versatile biocatalyst for the synthesis of chiral amines, we have analyzed the active site structure of ω -ATVf using homology modeling, and redesigned the enzyme. The homology modeling of ω -ATVf confirmed the previous results of its substrate structure-activity relationship. This indicated that the active site of ω -ATVf is consisted of one large and another small substrate-binding site. The key determinants in the

Table V. Substrate specificity of wild-type and mutant ω -ATVf toward substrate group III.

Substrate	Relative specific activity (μ_{rel} , %) ^a		
	W57G	W147G	Wild-type
C1 <chem>CC(C)N</chem>	69.1	21.9	3.6
C2 <chem>CCC(C)N</chem>	75.4	18.2	6.8
C3 <chem>CC(C)C(C)N</chem>	74.8	15.8	10.1
C4 <chem>CCCC(C)N</chem>	94.2	17.5	18.5
C5 <chem>CCCCCC(C)N</chem>	157.3	29.9	23.4
C6 <chem>CC(C)CCCC(C)N</chem>	357.8	34.8	24.4

^aThe reaction condition for the calculation of specific activity was as following: 0.1 mL of reaction media consists of 50 mM Tris-HCl (pH 7.2), 5 mM racemic amines, 10 mM pyruvate and 10 μ L cell-free synthesized wild-type and mutant ω -ATVf at 37°C. Relative specific activities (μ_{rel}) for amino donor were calculated based upon the specific activity for (S)-1-phenylethylamine.

recognition of the substrates appeared to be the differences in the size of each substrate-binding site, the electrostatic repulsion of carboxylate group of the substrates in the small substrate-binding site, and dual recognition mode for

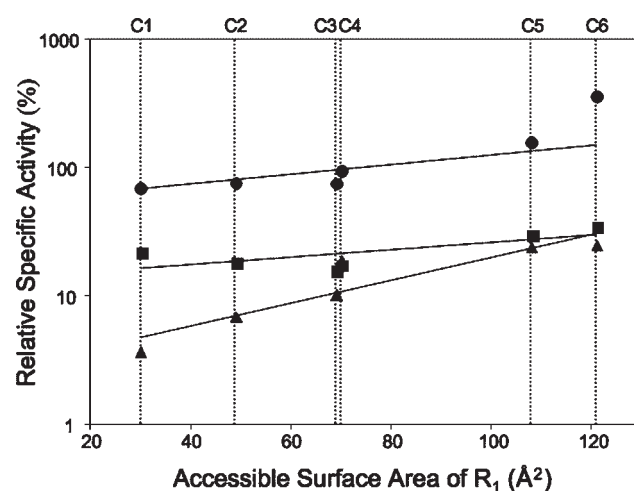


Figure 3. Relationships between the accessible surface area of substrate group III and the activity of the ω -ATVf (●, W57G ω -ATVf; ■, W147G ω -ATVf; ▲, wild-type ω -ATVf).

both hydrophobic and carboxylate groups in the large substrate-binding site. The dual substrate recognition mode of ω -ATVf could be explained by the existence of R264 in the large substrate-binding site and D21 in the small substrate-binding sites. R264 in the large substrate-binding site was predicted to interact with the α -carboxylate group of pyruvate instead of R415 in the small substrate-binding site, which is another conserved residue in all aminotransferases. The α -carboxylate group of pyruvate seemed to be located in the direction of the large substrate-binding site, because D21 possibly masked R415 residue and/or gave electrostatic repulsion with the α -carboxylate group of pyruvate. Interestingly, the R415K mutation in the small substrate-binding site of ω -ATVf resulted in the increase of the enzymatic activity toward the aromatic α -amino acids such as phenylglycine and phenylalanine. The homology modeling of ω -ATVf suggested that the negative correlation between the reactivities of aromatic amines and the accessible surface area of R1 might be caused by the strong hydrophobic interaction and/or the steric hindrance between the two tryptophan residues (i.e., W57 and W147) in the large binding subsite of ω -ATVf. The substitution of glycine for the tryptophan residues reduced the hydrophobic interaction thus allowing the enzyme to accept the bigger aromatic groups as well as the longer aliphatic chains. The fact that W57G mutation improved its catalytic activities for aromatic amines and for aliphatic amines without losing its original enantioselectivity suggested that the mutation allowed a more flexible conformation of the large substrate-binding site.

As shown in this study, the adaptation of an enzyme to new substrates is generally achieved by specificity relaxation in protein engineering (Chow et al., 2004). In the case of ω -ATVf, the specificity relaxation was carried out by a rational design based on the prediction of substrate recognition mode in the active site. The design principle can be primarily extracted from the known primary or secondary structure data. Additional 3D structural information of the enzyme of interest greatly helps to develop an advanced design principle to specifically pinpoint mutation sites, however 3D protein structures are not always available. We proposed the use of substrate specificity data in parallel with homology modeling to predict important residues for recognition of substrates. Simple correlation of the substrate specificity data with the structural information of the substrates (e.g., accessible surface area) provides a new insight into the design principles to improve our understanding of the proposed enzyme structure derived from the homology modeling. In conclusion, our results suggest that the design principle described herein can be applied to the stereospecific synthesis of other chiral amine compounds through broadening the substrate specificity of other transaminases.

This work was partially supported by the 21C Frontier Microbial Genomics and Applications, Center Programs from the Ministry of Science & Technology, and the Nano Bioelectronics & Systems Research Center in Seoul National University.

References

- Alexeeva M, Enright A, Dawson MJ, Mahmoudian M, Turner NJ. 2002. Deracemization of α -methylbenzylamine using an enzyme obtained by *in vitro* evolution. *Angew Chem Int Ed Engl* 41(17):3177–3180.
- Baker D, Sali A. 2001. Protein structure prediction and structural genomics. *Science* 294(5540):93–96.
- Balint J, Egri G, Czugler M, Schindler J, Kiss V, Juvancz Z, Fogassy E. 2001. Resolution of α -phenylethylamine by its acidic derivatives. *Tetrahedron: Asymmetry* 12(10):1511–1518.
- Chen R. 2001. Enzyme engineering: Rational redesign versus directed evolution. *Trends Biotechnol* 19(1):13–14.
- Cho BK, Cho HJ, Yun H, Kim B-G. 2003a. Simultaneous synthesis of enantiomerically pure (S)-amino acids and (R)-amines using α/ω -aminotransferase coupling reactions with two-liquid phase reaction system. *J Mol Catal B: Enzym* 26(3–6):273–285.
- Cho BK, Cho HJ, Park SH, Yun H, Kim BG. 2003b. Simultaneous synthesis of enantiomerically pure (S)-amino acids and (R)-amines using coupled transaminase reactions. *Biotechnol Bioeng* 81(7):783–789.
- Cho BK, Seo JH, Kang TW, Kim BG. 2003c. Asymmetric synthesis of L-homophenylalanine by equilibrium-shift using recombinant aromatic L-amino acid transaminase. *Biotechnol Bioeng* 83(2):226–234.
- Cho BK, Seo JH, Kang TJ, Kim J, Park HY, Lee BS, Kim BG. 2006. Engineering aromatic L-amino acid transaminase for the asymmetric synthesis of constrained analogs of L-phenylalanine. *Biotechnol Bioeng* 94(5):842–850.
- Chow MA, McElroy KE, Corbett KD, Berger JM, Kirsch JF. 2004. Narrowing substrate specificity in a directly evolved enzyme: The A293D mutant of aspartate aminotransferase. *Biochemistry* 43(40): 12780–12787.
- Eddy SR. 1998. Profile hidden Markov models. *Bioinformatics* 14(9):755–763.
- Eliot AC, Sandmark J, Schneider G, Kirsch JF. 2002. The dual-specific active site of 7, 8-diaminopelargonic acid synthase and the effect of the R391A mutation. *Biochemistry* 41(42):12582–12589.
- Gribskov M, McLachlan AD, Eisenberg D. 1987. Profile analysis: Detection of distantly related proteins. *Proc Natl Acad Sci USA* 84(13):4355–4358.
- Gutman AL, Meyer E, Kalerin E, Polyak F, Sterling J. 1992. Enzymatic resolution of racemic amines in a continuous reactor in organic solvents. *Biotechnol Bioeng* 40(7):760–767.
- Harel M, Sussman JL, Krejci E, Bon S, Chanal P, Massoulié J, Silman I. 1992. Conversion of acetylcholinesterase to butyrylcholinesterase—modeling and mutagenesis. *Proc Natl Acad Sci USA* 89(22):10827–10831.
- Hirotsu K, Goto M, Okamoto A, Miyahara I. 2005. Dual substrate recognition of aminotransferases. *Chem Rec* 5(3):160–172.
- Jewett MC, Swartz JR. 2004. Rapid expression and purification of 100 nmol quantities of active protein using cell-free protein synthesis. *Biotechnol Prog* 20(1):102–109.
- Kang TJ, Woo JH, Song HK, Ahn JH, Kum JW, Han J, Choi CY, Joo H. 2002. A cell-free protein synthesis system as an investigation tool for the translation stop processes. *FEBS Lett* 517(1–3):211–214.
- Kitaguchi H, Fitzpatrick PA, Huber JE, Klivanov AM. 1989. Enzymic resolution of racemic amines: Crucial role of the solvent. *J Am Chem Soc* 111(8):3094–3095.
- Kramer B, Rarey M, Lengauer T. 1999. Evaluation of the FLEXX incremental construction algorithm for protein-ligand docking. *Proteins* 37(2):228–241.
- Liu Y, Ruoho AE, Rao VD, Hurley JH. 1997. Catalytic mechanism of the adenylyl and guanylyl cyclases: Modeling and mutational analysis. *Proc Natl Acad Sci USA* 94(25):13414–13419.
- Liu W, Peterson PE, Carter RJ, Zhou X, Langston JA, Fisher AJ, Toney MD. 2004. Crystal structures of unbound and aminoxyacetate-bound *Escherichia coli* gamma-aminobutyrate aminotransferase. *Biochemistry* 43(34):10896–10905.
- Malashkevich VN, Onuffer JJ, Kirsch JF, Jansonius JN. 1995. Alternating arginine-modulated substrate specificity in an engineered tyrosine aminotransferase. *Nat Struct Biol* 2(7):548–553.

- Markova M, Peneff C, Hewlins MJ, Schirmer T, John RA. 2005. Determinants of substrate specificity in omega-aminotransferases. *J Biol Chem* 280(43):36409–36416.
- Marti-Renom MA, Stuart AC, Fiser A, Sanchez R, Melo F, Sali A. 2000. Comparative protein structure modeling of genes and genomes. *Ann Rev Biophys Biomol Struct* 29:291–325.
- Mehta PK, Hale TI, Christen P. 1993. Aminotransferases: Demonstration of homology and division into evolutionary subgroups. *Eur J Biochem* 214(2):549–561.
- Nicholas KB, Nicholas HB Jr., Deerfield DWI. 1997. GeneDoc: Analysis and Visualization of Genetic Variation. *EMBNEW NEWS* 4:14.
- Oehrner N, Orrenius C, Mattson A, Norin T, Hult K. 1996. Kinetic resolutions of amine and thiol analogs of secondary alcohols catalyzed by the *Candida antarctica* lipase B. *Enzyme Microb Technol* 19(5):328–331.
- Oue S, Okamoto A, Yano T, Kagamiyama H. 1999. Redesigning the substrate specificity of an enzyme by cumulative effects of the mutations of non-active site residues. *J Biol Chem* 274(4):2344–2349.
- Rarey M, Kramer B, Lengauer T, Klebe G. 1996. A fast flexible docking method using an incremental construction algorithm. *J Mol Biol* 261(3):470–489.
- Sheldon RA. 1996. Chirotechnology: Designing economic chiral syntheses. *J Chem Technol Biotechnol* 67(1):1–14.
- Shin JS, Kim BG. 1999. Asymmetric synthesis of chiral amines with omega-transaminase. *Biotechnol Bioeng* 65(2):206–211.
- Shin J-S, Kim B-G. 2002. Exploring the active site of amine:pyruvate aminotransferase on the basis of the substrate structure-reactivity relationship: How the Enzyme Controls Substrate Specificity and Stereoselectivity. *J Org Chem* 67(9):2848–2853.
- Shin JS, Yun H, Jang JW, Park I, Kim BG. 2003. Purification, characterization, and molecular cloning of a novel amine:pyruvate transaminase from *Vibrio fluvialis* JS17. *Appl Microbiol Biotechnol* 61(5–6):463–471.
- Siezen RJ, Devos WM, Leunissen JAM, Dijkstra BW. 1991. Homology modeling and protein engineering strategy of subtilases, the family of subtilisin-like serine proteinases. *Protein Eng* 4(7):719–737.
- Stemmer WPC. 2002. Molecular breeding of genes, pathways and genomes by DNA shuffling. *J Mol Catalysis B: Enzymatic* 19–20:3–12.
- Stewart JD. 2001. Dehydrogenases and transaminases in asymmetric synthesis. *Curr Opin Chem Biol* 5(2):120–129.
- Storici P, Capitani G, Muller R, Schirmer T, Jansonius JN. 1999. Crystal structure of human ornithine aminotransferase complexed with the highly specific and potent inhibitor 5-fluoromethylornithine. *J Mol Biol* 285(1):297–309.
- Taylor PP, Pantaleone DP, Senkpeil RF, Fotheringham IG. 1998. Novel biosynthetic approaches to the production of unnatural amino acids using transaminases. *Trends Biotechnol* 16(10):412–418.
- Thompson JD, Higgins DG, Gibson TJ. 1994. CLUSTAL W: Improving the sensitivity of progressive multiple sequence alignment through sequence weighting, position-specific gap penalties and weight matrix choice. *Nucleic Acids Res* 22(22):4673–4680.
- Tindbaek N, Svendsen A, Oestergaard PR, Draborg H. 2004. Engineering a substrate-specific cold-adapted subtilisin. *Protein Eng Des Sel* 17(2): 149–156.
- Yano T, Oue S, Kagamiyama H. 1998. Directed evolution of an aspartate aminotransferase with new substrate specificities. *Proc Natl Acad Sci USA* 95(10):5511–5515.
- Yun H, Hwang BY, Lee JH, Kim BG. 2005. Use of enrichment culture for directed evolution of the *Vibrio fluvialis* JS17 omega-transaminase, which is resistant to product inhibition by aliphatic ketones. *Appl Environ Microbiol* 71(8):4220–4224.